

perature of 3202°R will occur at an altitude of 233,200 ft. When the wing is swept 60°, the maximum leading-edge temperature is 2646°R and the maximum spherical-nose temperature is 3492°R. These temperatures differ from those calculated by the iterative procedure by less than 14°, which is an accuracy far greater than that inherent in the original calculated method of Ref. 1. Since the Re/ft range is from 4000 to 30,000 the assumption of laminar flow is well justified.

The preceding analysis assumes the vehicle to hold a constant altitude at each station of study. Along an inclined flight path with a resultant velocity U , with components u and v in the circumferential and radial directions, and with a resultant aerodynamic force inclined at an angle θ to the vertical, we have

$$T_w^4 = (868/\sigma) \{ [2g(1 + \delta)/\rho_0 U^2] \eta \lambda \}^{1/2} (10^{-8} U^2)^{1.575} \times \xi (B/R\epsilon^2)^{1/2} (\cos^{1.1} \Lambda_e) / 2^{1/2} \quad (11)$$

where

$$\delta = v^2/g(R_E + a) \text{ and } \lambda = (L/D)/[1 + (L/D)^2 \cos \theta]^{1/2}$$

The equations showing the velocity and altitude where the maximum possible temperature occurs become

$$U^2/(1 + \delta) = g\zeta \quad (12)$$

$$a = -(1/\beta) \ln \{ [2g(1 + \delta)/\rho_0 U^2] B \eta \lambda \} ft \quad (13)$$

Note that these equations in which the higher-order terms have been ignored are similar in form to Eqs. (4-6). If $\theta \approx 1^\circ$ ($v \approx 0.0175u$), the difference in calculated T_w introduced by neglecting these terms is less than 0.001%; if $\theta \approx 10^\circ$ ($v \approx 0.176u$), the difference is less than 0.05%.

With small error (well within the uncertainty of the reference calculation method), Eqs. (11-13) may be simplified to the following:

$$U/(1 + \delta)^{1/2} = 21,650 \text{ fps} \quad (14)$$

$$a = 233,200 - 23,500 \ln(10^{-2} B \lambda) ft \quad (15)$$

$$T_w = 3202(10^{-2} B/R\epsilon^2)^{1/8} (\cos^{0.275} \Lambda_e) (1 + \delta)^{0.394} \lambda^{1/8} R \quad (16)$$

and for the hemisphere nose

$$T_w = 3492(10^{-2} B/R\epsilon^2)^{1/8} (1 + \delta)^{0.394} \lambda^{1/8} R \quad (17)$$

Examination of Eqs. (14-17) shows that these are related to Eqs. (7-10) by the functions $(1 + \delta)$ and $\lambda = (L/D)/[1 + (L/D)^2 \cos \theta]^{1/2}$. For entry at a small θ with high L/D , these terms are near 1.0 and have little effect. For a rapid estimate of maximum equilibrium temperature, the results of Eq. (9) are presented in Fig. 1. For steeper descent, the temperature will be changed by the factor $(1 + \delta)^{0.394} \lambda^{1/8}$.

References

- 1 Detra, R. W., Kemp, N. H., and Riddell, F. R., "Addendum to Heat Transfer for Satellite Vehicle Re-Entering the Atmosphere," *Jet Propulsion*, Vol. 27, Dec. 1957, pp. 1256-1257.
- 2 Chapman, D. R., "An Approximate Analytical Method for Studying Entry Into Planetary Atmospheres," TR R-11, 1959, NASA.
- 3 Wisniewski, R. J., "Methods of Predicting Laminar Heat Rates on Hypersonic Vehicles," TN D-201, 1959, NASA.
- 4 Beckwith, I. E. and Gallagher, J. J., "Local Heat Transfer and Recovery Temperatures on a Yawed Cylinder at a Mach Number of 4.15 and High Reynolds Numbers," TR R-104, 1969, NASA.
- 5 *U.S. Standard Atmosphere*, NASA, U.S. Air Force, and U.S. Weather Bureau, Washington, D. C., 1962.

Flexibility Coefficients for Structural Joint Assemblies

SAUL M. KAPLAN*

General Electric Company, Schenectady, N. Y.

Introduction

THE sharp, localized reduction in effective modulus of rigidity (EI) across structural joint assemblies significantly influences the natural frequencies and mode shapes of launch vehicles, missiles, and spacecraft. The modular construction generally featured in unmanned spacecraft, for example, will result in structural joint flexibilities that can cumulatively reduce the natural frequencies associated with principal structural resonances by 10-25%.

Structural joint bending flexibility data have been published by Alley and Ledbetter.¹ Their empirical results, as shown in Fig. 1, present joint rotation constants, or bending flexibilities, as functions of: 1) the diameter of the structural joint assembly; and 2) the nature of joint construction. The four categories of joints—excellent, good, moderate, and loose—identified by Alley and Ledbetter, have their flexibility values presented as rather wide scatter bands. These structural joint flexibility data, while originally conceived as being applicable to multistage launch vehicles and missiles, have been successfully applied to a wide and diverse spectrum of other structures, including spacecraft, deployable spacecraft antennae, solar panels, and other complex spacecraft subsystems. Some high levels of correlation between structural dynamic analytical predictions and subsequent

REFERENCE: ALLEY, V. L., & LEDBETTER, S. A., "PREDICTION & MEASUREMENT OF NATURAL VIBRATIONS OF MULTISTAGE LAUNCH VEHICLES," *AIAA JOURNAL*, VOL. 1, NO. 2, PP. 374-379, FEBRUARY 1963.

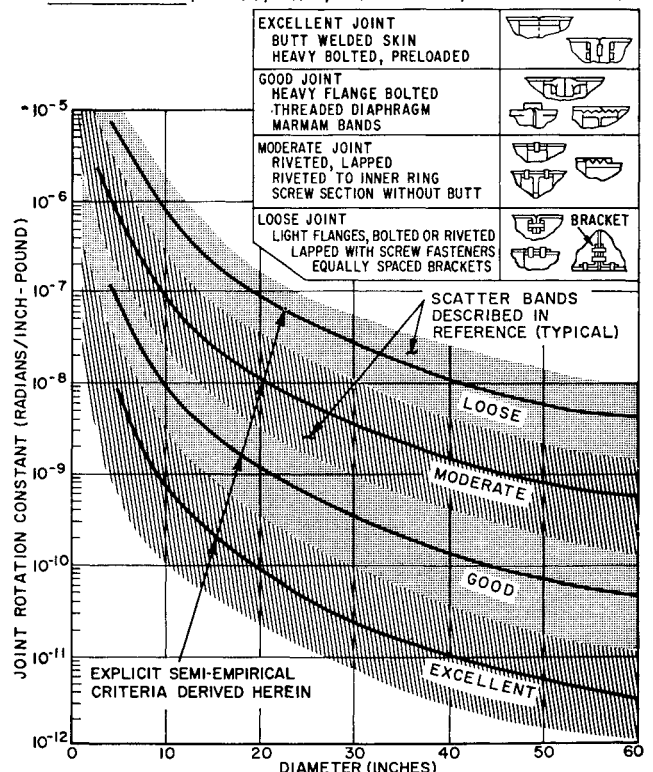


Fig. 1 Alley and Ledbetter's joint rotation constants.¹

Received October 8, 1970. This work was performed while the author was at the Company's Space Division, Valley Forge, Pennsylvania.

* Project Engineer. Gas Turbine Department.

test results² are largely attributed to the inclusion of these effects in analyses. Some means, however, must be found for defining the axial and torsional flexibilities across structural joint assemblies. (These are known to be significant factors for spacecraft applications.) In addition, conversion of the empirical Alley-Ledbetter data¹ into a semiempirical formulation will enhance its usefulness for future applications.

Semiempirical Bending Flexibility Coefficients

The empirical Alley-Ledbetter data¹ can be converted into a semiempirical formulation involving effective properties (denoted by the subscript *e*) of structural joint assemblies, through the relationship

$$\theta = M(L_e/EI_e) \quad (1)$$

For mated thin-walled structural elements, it follows that for a joint assembly having a nominal diameter *D*,

$$\theta = (M/D^3)(8L_e/\Pi t_e E_e) \quad (2)$$

The joint assembly modulus μ_e (units of in.²/lb) is defined by

$$\mu_e = 8L_e/\Pi t_e E_e \quad (3)$$

Substitution of Eq. (3) into Eq. (2) yields the semiempirical equation for the structural joint assembly bending flexibility coefficient:

$$C_B = \theta/M = \mu_e/D^3 \quad (4)$$

Values for μ_e (in.²/lb) can be extrapolated from the Alley-Ledbetter data¹ (Fig. 1). Recommended values are: a) loose joint, $7(10^{-4})$; b) moderate joint, $9(10^{-5})$; c) good joint $9(10^{-6})$; and d) excellent joint, $7(10^{-7})$. These semiempirical results, as evidenced by Fig. 1, fall in the middle of the empirical Alley-Ledbetter scatter bands for the entire range of diameters.

Semiempirical Axial and Torsional Flexibility Coefficients

Semiempirical axial and torsional flexibility coefficients can be likewise derived for structural joint assemblies. The axial flexibility coefficient C_A for thin-walled elements mated by a joint assembly of nominal diameter *D* is described by

$$C_A = \delta/P = L_e/\Pi t_e E D \quad (5)$$

Substitution for the joint assembly modulus μ_e from Eq. (3) into Eq. (5) yields

$$C_A = \mu_e/8D \quad (6)$$

The semiempirical torsional flexibility coefficient C_T is described by

$$C_T = \phi/T = L_e/JG \quad (7)$$

Taking $J = 2I$ and $G = E/2(1 + \nu)$, it follows that

$$C_T = (8L_e/E\Pi t_e)(1 + \nu)/D^3 \quad (8)$$

Substitution of Eq. (3) into the Eq. (8) yields

$$C_T = [(1 + \nu)\mu_e]/D^3 \quad (9)$$

The previously cited values of μ_e as a function of joint category apply to the axial and torsional flexibility coefficient equations as well.

Conclusions

Semiempirical formulations have been established for representing the bending, axial, and torsional flexibility coefficients for structural joint assemblies. These expressions show joint flexibility to be inversely proportional to the cube of the joint assembly diameter for the bending and torsional cases, and inversely proportional to this diameter for the axial case. [The torsional case also shows a direct proportionality to Poisson's ratio in a $(1 + \nu)$ form.] The

constants of proportionality are the same in each expression; different constants are required—and have been defined herein—for the four categories of structural joints identified by Alley and Ledbetter.¹ These results are necessary ingredients for, and can be applied directly in, spacecraft system and subsystem structural dynamic analyses.

References

- ¹ Alley, V. L. and Ledbetter, S. A., "Predictions and Measurement of Natural Vibrations of Multi-Stage Launch Vehicles," *AIAA Journal*, Vol. 1, No. 2, Feb. 1963, pp. 374-379.
- ² Kaplan, S. M. and Terkun, V., "Dynamic Analysis of the ATS-B Spacecraft," *Shock and Vibration Bulletin*, Vol. 39, No. 7, Feb. 1967, pp. 41-62.

A Solid-Propellant Rocket Motor Modulated by a Fluidic Vortex Valve

R. F. WALSH,* W. S. LEWELLEN,†
AND D. B. STICKLER‡

Massachusetts Institute of Technology,
Cambridge, Mass.

Nomenclature

<i>a</i>	= burning rate constant ($\dot{r} = aP_s^n$)
<i>A_c</i>	= control port area
<i>A_{eff}, A_t</i>	= effective and geometric throat areas
<i>M_c, M_s</i>	= control and supply gas molecular weights
<i>n</i>	= burning rate pressure exponent ($\dot{r} = aP_s^n$)
<i>P_s</i>	= combustion chamber stagnation pressure
\dot{r}	= propellant linear regression rate = aP_s^n
<i>r_t</i>	= nozzle throat radius
<i>r_w</i>	= vortex valve chamber radius
<i>T_c, T_s</i>	= control gas and combustion chamber stagnation temperatures
<i>W_c, W_s</i>	= control and supply (propellant) mass flow divided by the maximum possible nozzle flow for the same chamber stagnation conditions
<i>W₀</i>	= normalized total nozzle flow = $W_c + W_s$
β, η	= A_{eff}/A_t and W_c/W_s , respectively

Introduction

THIS investigation was undertaken to determine the basic feasibility of modulating the burning rate of a solid propellant rocket by using a fluidic vortex valve (VV) controlled by a small auxiliary motor (Fig. 1). Nelson et al.¹ tested several VV-controlled rocket motors (VVRMs). They usually incorporated a bypass orifice to parallel the VV. The present arrangement differs from theirs in that the valve provides the only exhaust path. Keranen and Blatter² studied the effects of combustion gases from aluminized propellants on internal VV components. In their push-pull VVRM, they maintained a constant combustion pressure,

Presented as Paper 70-643 at the AIAA 5th Propulsion Joint Specialist Conference, San Diego, Calif., June 15-19, 1970; submitted July 6, 1970; revision received October 29, 1970. The authors acknowledge Atlantic Research Corporation for their assistance in providing propellants for the experimental portion of this work.

* NSF Graduate Fellow, Department of Aeronautics and Astronautics; now Member of the Technical Staff at Rocketdyne, Calif., Member AIAA.

† Associate Professor, Department of Aeronautics and Astronautics. Member AIAA.

‡ Assistant Professor, Department of Aeronautics and Astronautics. Member AIAA.